

Ion sensors based on organic semiconductors acting as quasi-reference electrodes

Yu Yamashita^{a,b,1}, Harumi Hayakawa^a, Pushi Wang^a, Tatsuyuki Makita^a, Shohei Kumagai^{a,1,2}, Shun Watanabe^a, and Jun Takeya^{a,b}

Thin-film devices that transduce the chemical activity of ions into electronic signals are essential components in various applications, including healthcare diagnostics and environmental monitoring. Combinations of organic semiconductors (OSCs) and ion-selective materials have been explored for developing solution-processable ion sensors. However, the necessity of reference electrodes and operational stability in ion-permeable OSCs have posed questions regarding whether reliable measurements with thin-film components are attainable with OSCs. Herein, we report electric double-layer transistors (EDLTs) with OSCs in single-crystal forms for ion sensing. Our EDLTs demonstrated high operational stability, with a one-to-one relationship between the source electrode potential and device resistance, and served as quasi-reference electrodes. When our EDLT is served as quasi-reference electrode, its drift was as small as 0.5 mV/h and comparable to that of commonly employed reference electrodes. In our system, the semiconductor-electrolyte interface is self-passivated by the alkyl chains of OSCs in single-crystal structures, with the two-dimensional transport layer appearing unaltered upon gating. EDLT arrays with ion-selective and non-selective liquid junctions enable ion concentration sensing without a conventional reference electrode. These findings provide opportunities to develop thin-film devices based on OSCs for easy integration and reliable measurements.

organic semiconductor | ion sensor | electric double layer transistor

Introduction High-resolution, real-time, and easy-to-use measurements of ion activity in analytes are crucial in various biochemical applications, ranging from healthcare diagnostics to environmental monitoring(1, 2). Potentiometric ion sensing(3), which converts the difference in ionic activity to a difference in electric potential using an ion-selective membrane (ISM), provides a portable sensing platform. Potentiometric ion sensors commonly employ a reference electrode (RE) that is bulky, expensive, and requires a large sample volume, which does not meet the requirements of looming thin-film sensor applications. The demand for miniaturized ion sensors has led to the development of solid-state ion sensors represented by ion-sensitive field-effect transistors (ISFETs)(4, 5), in which an ISM is fabricated adjacent to a semiconductor. However, REs are commonly required to precisely control the gate voltages of ISFETs. Attempts to fabricate REs in thin-film configurations have been reported; however, their accuracy and lifetime still need to be improved(6). Replacing REs with reference transistors is another proposed approach for fabricating miniaturized sensors in which differential measurements between the reference and ion-sensing transistors have been conducted(7–10). Reference transistors that demonstrate stable resistance to changes in ion activities have been sought by passivating ISFET surfaces with ion-insensitive materials such as insulating polymers(11, 12). Thus far, issues such as ion diffusion inside insulating polymers have hindered mV-scale reliable measurements in these systems, making fabrication and application of reference transistors has remained a longstanding challenge.

To fabricate low-drift transistors that may serve as a reliable reference, a stable solid-liquid interface must be developed(13–15). Thus, inorganic insulators, such as silicon oxides and silicon nitrides, are not ideal because of their susceptibility to chemical modification of surfaces in aqueous solutions(16). Compared to most inorganic materials that are susceptible to chemisorption processes, closed-shell molecules without dangling bonds may provide more stable solid-liquid interfaces. Using organic semiconductors (OSCs) as the active layers of transistors(17–20) is a facile way to fabricate devices without materials that are susceptible to chemisorption processes in aqueous environments. However, while the chemical structures of OSCs are stable even in aqueous environments(21–23), most OSC thin films are ion-permeable, and thin-film structures are irreversibly altered

Significance Statement

Thin-film ion sensors are demanded for a wide range of biochemical-sensing applications. While transistors based on inorganic and organic semiconductors have been studied for this purpose, conventional ion-sensing transistors require the use of a bulky reference electrode such as Ag/AgCl. Therefore, the central problem of ion sensor miniaturization has not yet been addressed. In this study, single crystals of an organic semiconductor were used in electric double-layer transistors to develop ion sensors. Owing to their unique operational stability, the fabricated transistors realized one-to-one conversion of current levels and electrode potentials, that is, they served as quasi-reference electrodes. Differential measurements between the thin-film sensing and reference transistors enabled facile and reliable ion sensing, which eliminated conventional reference electrodes.

Author affiliations: ^aMaterial Innovation Research Center (MIRC) and Department of Advanced Material Science, Graduate School of Frontier Science, The University of Tokyo, 5-1-5 Kashiwanoha, Kashiwa, Chiba 277-8561, Japan; ^bResearch Center for Materials Nanoarchitectonics (MANA), National Institute for Materials Science (NIMS), 1-1 Namiki, Tsukuba, Ibaraki 305-0044, Japan

Y.Y. conceived of measurement principles. H. H., T. M., and S. K. conducted device fabrications and measurements. P. W. evaluated stability of devices. Y.Y. and S. K. wrote the manuscript. S.W. and J.T. supervised the work.

The authors declare no competing financial interests.

¹To whom correspondence may be addressed. Email: YAMASHITA.Yu@nims.go.jp, kumagai.s.am@m.titech.ac.jp ²Current address: Department of Chemical Science and Engineering, School of Materials and Chemical Technology, Tokyo Institute of Technology, 4259-G1-7 Nagatsuta, Midori-ku, Yokohama 226-8502, Japan.

through electrochemical transistor operations(24, 25). In structurally disordered OSCs, the Fermi energy is pinned to localized states(26), which limits the operational stability of electrochemical transistors based on OSCs.

In this study, we demonstrate thin-film ion sensors based on organic electric double-layer transistors (EDLTs) without using an RE. The concept of the proposed system is illustrated in Fig. 1a. In conventional systems, an RE is employed with a sensor transistor that bears ion-selective membranes. In our system, the RE was replaced with a reference EDLT composed of the same single-crystal form of solution-processed small-molecule OSC employed for sensing EDLTs. A stable resistance value at a given source-electrode potential is observed in the reference EDLT. Such a one-to-one conversion of the Fermi energy and resistance is established with a system close to the degenerate limit, where a sharp increase in transistor operation suggests a low density of trap states. Owing to the operational reliability of EDLT, a resistance measure provides an accurate source electrode potential without using an RE, which allows this EDLT to serve as a quasi-reference electrode (qRE). Through differential measurements between a reference EDLT and an EDLT bearing a potassium ion-selective membrane, selective sensing of potassium ions is realized with sensitivity approaching the Nernst limit. The observed operational stability is likely to rise from the unique solid-liquid interface in our devices, where the surface of the two-dimensional hole transporting layer is passivated by alkyl chains in the single-crystal structure of OSC. These results suggest that the single crystals of OSCs are suitable materials for fabricating electrochemical sensors and biosensors in thin-film configurations.

Electric Double-Layer Transistors based on Organic Thin-Film Single Crystal

This study examines EDLTs based on thin-film single crystals (TFSCs) of OSC, which can be made into an all-in-film structure shown in Fig. 1b. One of the benchmarked OSC, 3,11-dinonyldinaphtho[2,3-d:2',3'-d']benzo[1,2-b:4,5-b']dithiophene (C9-DNBDT-NW), was employed to leverage its suitability for manufacturing large and few molecules-thick TFSCs by solution-coating technique with high reproducibility(27). Solution-grown TFSCs of C9-DNBDT-NW were patterned on a substrate with bottom-contact source and drain electrodes. To fabricate the all-in-film device, a bank structure made of 500 μm -thick polydimethylsiloxane (PDMS) was filled with inner filling solution (IFS) containing 0.1 M K_2SO_4 and polyvinylpyrrolidone. This IFS was covered with a non-ionselective liquid junction membrane in this measurement. The EDLT properties were investigated in an aqueous K_2SO_4 gate electrolyte (0.1 M) in the presence of an Ag/AgCl reference electrode (See Supplementary Information Section 1 for detailed methods). Fig. 1c is an illustration of the potential across the device, where the electric double layers at the gate/electrolyte and OSC/electrolyte interfaces cause drops in the electric potential Φ . The electrochemical potential of electrons (Fermi energy) is plotted as $\bar{\mu}_e$. As shown in Fig. 1d, a typical p-channel EDLT operation was observed when gate voltage (V_g) was controlled using Ag/AgCl while applying a constant drain voltage (V_d) of -0.05 V. Here, I_d

was plotted against V_{ref} which is defined as the electrode potential difference between the source and Ag/AgCl. Interestingly, the subthreshold swing of 75 mV dec^{-1} was close to the theoretical limit at room temperature (59 mV dec^{-1}) and significantly smaller than that reported for organic EDLTs or electrochemical transistors based on polymeric semiconductors ($>200 \text{ mV dec}^{-1}$)(28, 29), which suggests the low trap density of states in TFSCs.

To evaluate the operational stability of our device, I_d was measured while V_{ref} was fixed at -0.55 V using the gate and Ag/AgCl electrodes. The EDLT exhibited a stable I_d after a steady state was established within an hour, where the I_d drift was only -0.3 nA/h (Fig. 1e). Considering that sensors based on electrochemical transistors with ion-permeable polymeric semiconductors are typically tested at a timescale of 10 min, an EDLT based on a TFSC realizes significantly improved stability. The observed I_d drift corresponds to a drift in the threshold voltage of approximately 0.5 mV/h , which is actually comparable to that of commonly employed reference electrodes(30). The observed drifts in I_d may arise from our EDLT or the RE employed in this measurement.

The observed operational stability suggested that the EDLT based on OSC TFSC served as a qRE. In an EDLT, the amount of charge accumulated on the surface of OSC depends on the potential drop at the electrolyte/OSC interface, which is defined as the effective gate voltage ($V_{g,\text{eff}}$). This value was equal to V_{ref} in the above measurements. The observed stable I_d at a constant $V_{g,\text{eff}}$ suggests that the mobility and trap density of states did not change during the measurement, and the single-crystal structure should be maintained similarly to our previous studies in non-aqueous environments(31, 32). In a single-crystal structure(33), the two-dimensional carrier transporting layer is self-passivated by the alkyl chains from the electrolytes, which is beneficial for stable EDLT operations in aqueous solutions. Consequently, I_d and $V_{g,\text{eff}}$ exhibit a one-to-one relationship, where the measure of I_d provides an accurate value of $V_{g,\text{eff}}$ that equals V_{ref} . In the following sections, we demonstrate replacement of bulky REs in ion sensing devices with our thin-film EDLTs.

Aqueous ion sensing using EDLT bearing ion-selective membranes

Conventional potentiometric ion sensors are composed two REs separated by an ion-selective membrane (ISM). In the following, first, we demonstrate replacement of one of the REs with our EDLT. To develop ion sensing devices based on the EDLTs, ISMs were employed to separate the analyte and IFS. Fig. 2a shows an illustration of the potential across the device bearing an ISM. An ISM develops a membrane potential $\Delta\Phi_{\text{ISM}}$ that depends on difference in concentrations of the target ion between the analyte and IFS, where evaluation of $\Delta\Phi_{\text{ISM}}$ is required to determine the concentration of the target ion. Here, we preliminarily demonstrate K^+ sensing using valinomycin(34, 35) as a K^+ ionophore in the ISM. In this case, the concentration of K^+ was varying in the analyte while that in the IFS was constant. Ag/AgCl was used in the analyte and IFS for the device operation and verification of the working mechanism, for which purpose the EDLT was built in a small container filled with the IFS. See method section and supplementary information Section

1 for details of device preparation. To test responses of the device to the ion concentrations, transfer curves were acquired at different $[K^+]$ values in the analyte, during which the gate electrode was placed in the analyte (Fig. 2b). The obtained transfer curves showed a threshold voltage (V_{th}) shift toward positive V_g values with decreasing $[K^+]$. In this measurement, the applied V_g should be divided at the gate electrode/analyte interface, the ISM, and the IFS/OSC interface as shown in Fig. 2a. At a smaller $[K^+]$, the potential shift at the ISM ($\Delta\Phi_{ISM}$) should have increased, resulting in an increased $V_{g,eff}$. Linear fitting of the on states (dashed lines) afforded comparable slopes, indicating a unique hole mobility for varying $[K^+]$. Indeed, the transfer curves were almost identical when plotted against $V_{ref,in}$, which is the electrode potential difference between the source and Ag/AgCl placed in the IFS (Fig. 2c). This suggests that the EDLT responds to $V_{g,eff}$ for all the obtained conditions in an identical manner, which is consistent with the qRE operation of OSC TFSCs.

Ion sensing was demonstrated by monitoring I_d of the EDLT bearing K^+ ISM while changing the $[K^+]$ of the analyte. In this measurement, we employed a gate electrode, an Ag/AgCl RE, and the EDLT bearing K^+ ISM immersed in analyte solutions. Note that analyte solutions contained Na^+ that serves as an interfering ion, where $[Na^+] + [K^+]$ was constant for all conditions. For the case without an interfering ion, see Supplementary Information Fig. S1. In the measurement shown in Fig. 2d, constant V_g of -0.4 V and V_d of -0.1 V were employed. $V_{ref,out}$ during this measurement is shown in Supplementary Information Fig. S2. Here, $V_{ref,in}$, which is equal to $V_{g,eff}$, can be estimated from I_d and the transfer characteristics (Supplementary Information Fig. S3). $[K^+]$ was calculated from the $\Delta\Phi_{ISM}$, which can be deduced from the following equation: $\Delta\Phi_{ISM} = V_{ref,out} - V_{g,eff}$ (Fig. 2e). The slope in the linear region was calculated as 61 mV dec^{-1} , which is consistent with the Nernstian response. This result demonstrates selective and reliable responses of our EDLT bearing K^+ ISM to $[K^+]$ in the analyte.

Reliable ion sensing is not limited to K^+ in our system. In another example, NH_4^+ sensing has been demonstrated by employing nonactin (36, 37) as the ionophore. Using the same procedure as that for K^+ sensing, I_d for varying $[NH_4^+]$ was obtained (Fig. 3a) and employed to estimate $\Delta\Phi_{ISM}$ (Fig. 3b). The slope in the linear region (dashed line) was calculated to be 44 mV dec^{-1} , which is slightly smaller than an ideal Nernstian response. Tuning the composition of the ISM and IFS may improve sensitivity. The above measurements suggest that EDLTs based on OSC TFSCs provide a platform for ion sensing when combined with various ISMs owing to the operational and environmental stability of the material.

Aqueous ion sensing by all-in-film organic TFSC EDLTs

Finally, aqueous K^+ sensing was demonstrated using a pair of all-in-film EDLTs acting as the sensing EDLT and reference EDLT, which realizes ion sensing without bulky REs. K^+ ISM was employed as the liquid junction of the

sensing EDLT, whereas a non-ion-selective liquid junction was employed for the reference EDLT. A planar thin-film Au gate electrode was employed during the ion sensing measurement, which is fabricated on the same substrate as the EDLT. Fig. 4a shows an illustration of the potentials across the device. At the interface of analyte/IFS, there should be a negligible drop in the electric potential for the reference EDLT owing to ionic conductivity and non-selectivity of the employed liquid junction. In this situation, the potential drop at ISM can be estimated based on the $V_{g,eff}$ of reference and sensing EDLTs: $\Delta\Phi_{ISM} = V_{g,eff}^{ref} - V_{g,eff}^K$. Fig. 4b shows monitored I_d for varying $[K^+]$. In this experiment, V_g was controlled such that I_d for the reference EDLT (I_d^{ref}) became constant, which is expected to keep $V_{g,eff}$ constant for the reference EDLT. When the reference EDLT serves as qRE, this measurement condition is equivalent to that in which V_g was controlled to produce a constant V_{ref} by employing an RE in the analyte. In this case, measurements of I_d^K is enough to evaluate $[K^+]$. In order to convert I_d^K into $V_{g,eff}$, the transfer curve that serves as a calibration curve was measured before the ion sensing measurements using an RE (Fig. 4c). Based on the I_d^K plotted in Fig. 4c and the calibration curve plotted in Fig. 4d, $V_{g,eff}^K$ and $\Delta\Phi_{ISM}$ (Fig. 4d) were evaluated. The slope in the linear region in the plot of $\Delta\Phi_{ISM}$ was 62 mV dec^{-1} , which is close to the Nernstian response and demonstrates successful ion sensing using the pair of EDLTs. This successful evaluation owes to stability of our EDLTs during this measurements. To achieve small drifts of EDLTs in a longer time scale, proper choice of initial aging time and measurement conditions would be important, which is discussed in Fig. S5 and S6 and studied further in future research.

In this study, OSC TFSCs were employed as the active layers of EDLTs, which achieved dramatically improved operational stability compared with conventional organic electrochemical transistors. Our EDLT demonstrated a one-to-one conversion between the drain currents and effective gate voltages, which allowed the device to serve as a qRE. In our TFSCs, the interface between the electrolyte and carrier-transporting layer was self-passivated by alkyl chains, which is likely to be the key to qRE operations. Ion-selective responses were established by combining ISMs with our EDLTs. Differential measurements of the reference and sensing EDLTs enabled ion sensing without using a conventional RE. Our findings will lead to OSC-based thin-film devices that feature reliability and easy integration for electrochemical and biochemical sensing applications.

Methods

Fabrication of PET films with liquid junctions: Valinomycin was employed as the K^+ ionophore(38). Nonactin was employed as NH_4^+ ionophore(5). PET films with around a-few-millimeter holes are prepared, to which solutions for ISM or ion-nonselective liquid junction were drop casted.

Fabrication of an EDLT inside a container filled with IFS :125 μm -thick PEN films with 200 nm-thick parylene (diX-SR) layers were employed as substrates. Source and drain electrodes were thermally deposited as 20 nm-thick Au electrodes. Solution-processed TFSCs of C9-DNBDT-NW were transferred to the PEN substrates with the c-axis of

the TFSC parallel to the source-drain direction(39). The fabricated EDLT device was installed into a cylinder-shaped container made of polypropylene and PEN that is filled with aqueous IFS. PET films with liquid junctions were installed to this container so that IFS and analyte are separated by the liquid junctions. Note that an RE can be inserted inside or outside of the liquid junction for this device structure.

Fabrication of an all-in-film EDLT: Souce/drain electrodes and TFSCs of C9-DNBDT-NW were fabricated on PEN substrates in the same method as the EDLTs inside a container filled with IFS. 500 μm -thick PDMS films in a bank structure were placed on the EDLT devices. This bank structure was filled with 0.1 M K_2SO_4 aqueous solution with 10 wt% polyvinylpyrrolidone that serves as an IFS. PET films with liquid junctions were placed on top to confine the IFS.

See supplementary information for further details of materials, device fabrications, and employed electrolytes.

1. L Burton, K Jayachandran, S Bhansali, The “Real-Time” revolution for in situ soil nutrient sensing. *J. The Electrochem. Soc.* **167**, 037569 (2020).
2. T Ozer, I Agir, CS Henry, Low-cost Internet of Things (IoT)-enabled a wireless wearable device for detecting potassium ions at the point of care. *Sensors Actuators B: Chem.* **365**, 131961 (2022).
3. JT Stock, MV Orna, et al., *Electrochemistry, past and present*. (ACS Publications) Vol. 390, (1989).
4. S Martinoa, G Massobrio, L Lorenzelli, Modeling ISFET microsensor and ISFET-based microsystems: a review. *Sensors Actuators B: Chem.* **105**, 14–27 (2005).
5. I Fakih, et al., Selective ion sensing with high resolution large area graphene field effect transistor arrays. *Nat. Commun.* **11**, 3226 (2020).
6. M Sophocleous, JK Atkinson, A review of screen-printed silver/silver chloride (ag/agcl) reference electrodes potentially suitable for environmental potentiometric sensors. *Sensors Actuators A: Phys.* **267**, 106–120 (2017).
7. U Guth, F Gerlach, M Decker, W Oelßner, W Vonau, Solid-state reference electrodes for potentiometric sensors. *J. Solid State Electrochem.* **13**, 27–39 (2009).
8. H Nakajima, M Esashi, T Matsuo, The Cation Concentration Response of Polymer Gate ISFET. *J. The Electrochem. Soc.* **129**, 141 (1982).
9. M Milgrew, P Hammond, D Cumming, The development of scalable sensor arrays using standard cmos technology. *Sensors Actuators B: Chem.* **103**, 37–42 (2004).
10. N Moser, L Keeble, J Rodriguez-Manzano, P Georgiou, ISFET arrays for lab-on-chip technology: A review in 2019 26th IEEE International Conference on Electronics, Circuits and Systems (ICECS). (IEEE), pp. 57–60 (2019).
11. E Salm, et al., Electrical Detection of Nucleic Acid Amplification Using an On-Chip Quasi-Reference Electrode and a PVC REFET. *Anal. Chem.* **86**, 6968–6975 (2014).
12. KM Chang, CT Chang, KY Chao, JL Chen, Development of FET-Type Reference Electrodes for pH-ISFET Applications. *J. Electrochem. Soc.* **157**, J143 (2010).
13. Y Sasaki, H Kwarada, Low drift and small hysteresis characteristics of diamond electrolyte-solution-gate fet. *J. Phys. D: Appl. Phys.* **43**, 374020 (2010).
14. W Wei, W Liao, Z Zeng, C Zhu, Extended Gate Reference-FET (REFET) Using 2D h-BN Sensing Layer for pH Sensing Applications. *IEEE Electron Device Lett.* **41**, 159–162 (2019).
15. G Parish, et al., Role of GaN cap layer for reference electrode free AlGaIn/GaN-based pH sensors. *Sensors Actuators B: Chem.* **287**, 250–257 (2019).
16. S Jamasb, S Collins, RL Smith, A physical model for drift in ph isfets. *Sensors Actuators B: Chem.* **49**, 146–155 (1998).
17. J Rivnay, et al., Organic electrochemical transistors. *Nat. Rev. Mater.* **3**, 1–14 (2018).
18. M Sessolo, J Rivnay, E Bandiello, GG Malliaras, HJ Bolink, Ion-Selective Organic Electrochemical Transistors. *Adv. Mater.* **26**, 4803–4807 (2014).
19. F Torricelli, et al., Electrolyte-gated transistors for enhanced performance bioelectronics. *Nat. Rev. Methods Primers* **1**, 66 (2021).
20. Y Yao, et al., Flexible and Stretchable Organic Electrochemical Transistors for Physiological Sensing Devices. *Adv. Mater.* p. 2209906 (2023).
21. CB Nielsen, et al., Molecular design of semiconducting polymers for high-performance organic electrochemical transistors. *J. Am. Chem. Soc.* **138**, 10252–10259 (2016).
22. A Giovannitti, et al., N-type organic electrochemical transistors with stability in water. *Nat. Commun.* **7**, 13066 (2016).
23. LR Savagian, et al., Balancing Charge Storage and Mobility in an Oligo(Ether) Functionalized Dioxithiophene Copolymer for Organic- and Aqueous- Based Electrochemical Devices and Transistors. *Adv. Mater.* **30**, 1804647 (2018).
24. JT Friedlein, et al., Influence of disorder on transfer characteristics of organic electrochemical transistors. *Appl. Phys. Lett.* **111**, 023301 (2017).
25. A Savva, et al., Influence of Water on the Performance of Organic Electrochemical Transistors. *Chem. Mater.* **31**, 927–937 (2019).
26. S Wang, M Ha, M Manno, C Daniel Frisbie, C Leighton, Hopping transport and the hall effect near the insulator–metal transition in electrochemically gated poly (3-hexylthiophene) transistors. *Nat. Commun.* **3**, 1210 (2012).
27. S Kumagai, T Makita, S Watanabe, J Takeya, Scalable printing of two-dimensional single crystals of organic semiconductors towards high-end device applications. *Appl. Phys. Express* **15**, 030101 (2022).
28. L Kergoat, et al., A Water-Gate Organic Field-Effect Transistor. *Adv. Mater.* **22**, 2565–2569 (2010).
29. D Wang, V Noël, B Piro, Electrolytic gated organic field-effect transistors for application in biosensors—A review. *Electronics* **5**, 9 (2016).
30. MP Mousavi, SA Saba, EL Anderson, MA Hillmyer, P Buhlmann, Avoiding Errors in Electrochemical Measurements: Effect of Frit Material on the Performance of Reference Electrodes with Porous Frit Junctions. *Anal. Chem.* **88**, 8706–8713 (2016).
31. S Watanabe, et al., Surface Doping of Organic Single-Crystal Semiconductors to Produce Strain-Sensitive Conductive Nanosheets. *Adv. Sci.* **8**, 2002065 (2021).
32. N Kasuya, J Tsurumi, T Okamoto, S Watanabe, J Takeya, Two-dimensional hole gas in organic semiconductors. *Nat. Mater.* **20**, 1401–1406 (2021).
33. T Okamoto, et al., Bent-shaped p-type small-molecule organic semiconductors: A molecular design strategy for next-generation practical applications. *J. Am. Chem. Soc.* **142**, 9083–9096 (2020).
34. Y Alifragis, et al., Potassium selective chemically modified field effect transistors based on AlGaIn/GaN two-dimensional electron gas heterostructures. *Biosens. Bioelectron.* **22**, 2796–2801 (2007).
35. T Ji, P Rai, S Jung, VK Varadan, In vitro evaluation of flexible pH and potassium ion-sensitive organic field effect transistor sensors. *Appl. Phys. Lett.* **92**, 208 (2008).
36. M Cuartero, N Colozza, BM Fernández-Pérez, GA Crespo, Why ammonium detection is particularly challenging but insightful with ionophore-based potentiometric sensors—an overview of the progress in the last 20 years. *Analyst* **145**, 3188–3210 (2020).
37. ST Keene, et al., Wearable organic electrochemical transistor patch for multiplexed sensing of calcium and ammonium ions from human perspiration. *Adv. healthcare materials* **8**, 1901321 (2019).
38. J Bobacka, Potential stability of all-solid-state ion-selective electrodes using conducting polymers as ion-to-electron transducers. *Anal. chemistry* **71**, 4932–4937 (1999).
39. T Makita, et al., Nano-Ground Glass as a Superhydrophilic Template for Printing High-Performance Organic Single-Crystal Thin Films. *Adv. Mater. Interfaces* **8**, 2100033 (2021).

Acknowledgments

This work was supported in part by JSPS KAKENHI grants (nos. JP20H00392, JP22H04959). This work was supported in part by JST, CREST Grant Number JPMJCR21O3.

Data availability

The data supporting the plots within this study are available from Zenodo at <https://doi.org/10.5281/zenodo.13132262>.

Supplementary materials

Materials and Methods

Figs. S1 to S6

References

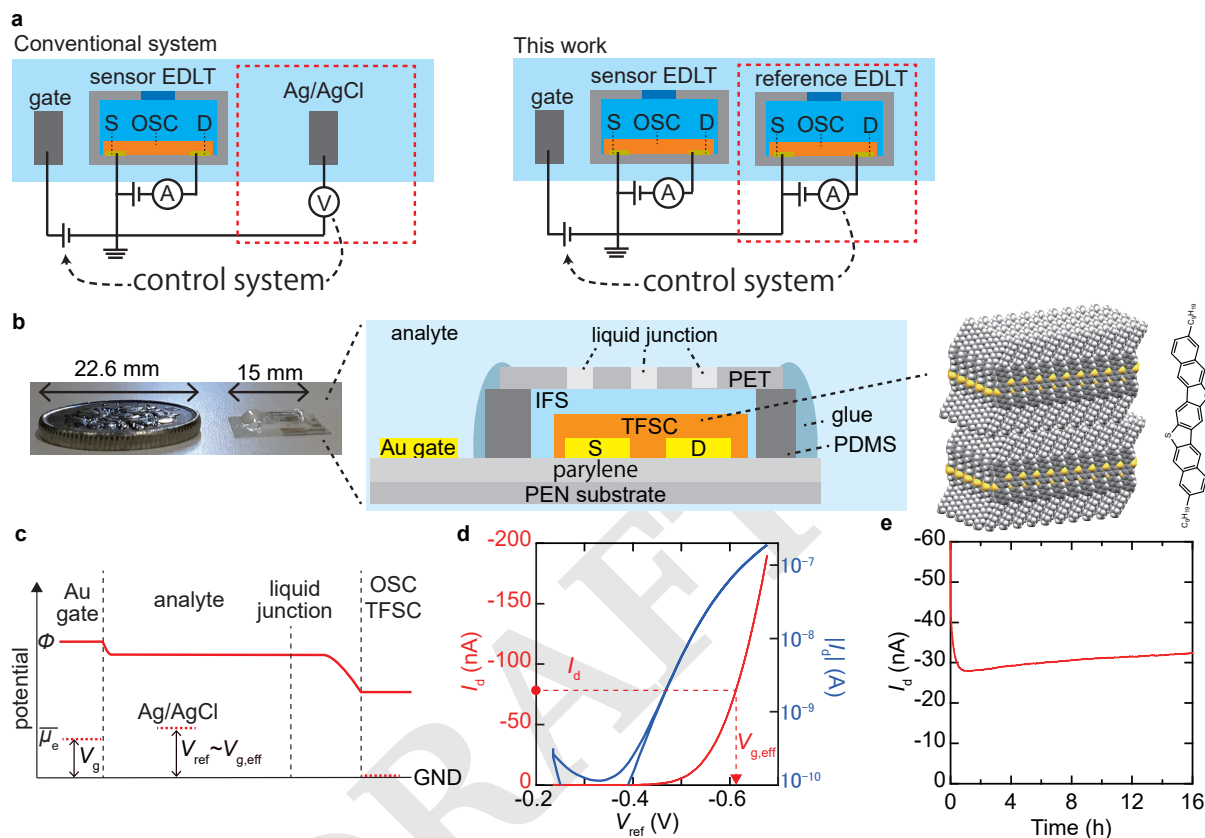


Fig. 1. Proposed principle of qRE based on OSC TFSCs. (a) Illustration of the conventional and our measurement systems. S and D denotes source and drain electrodes respectively. While gate voltage is controlled using an Ag/AgCl in a conventional three-electrode system, it was controlled using a reference EDLT in our system. (b) A photo and an illustration of the fabricated all-in-film device together with the chemical and crystal structures of C9-DNBDT-NW. (c) Illustration of a potential diagram of an EDLT with a non-ionselective liquid junction. Electric potential Φ is shown in a solid line and the electrochemical potential of electrons μ_e (Fermi energy) is shown in dashed lines. GND denotes the ground level of the system, which equals to the source electrode potential. (d) Transfer characteristics of an EDLT in linear (red) and log (blue) scales, where Ag/AgCl was employed during the measurement similar to the conventional system. V_d was -0.05 V and V_g sweep rate was 0.01 V / 10 sec. (e) Operational stability of an EDLT under V_{ref} of -0.55 V and V_d of -0.05 V, where Ag/AgCl was employed to keep V_{ref} constant.

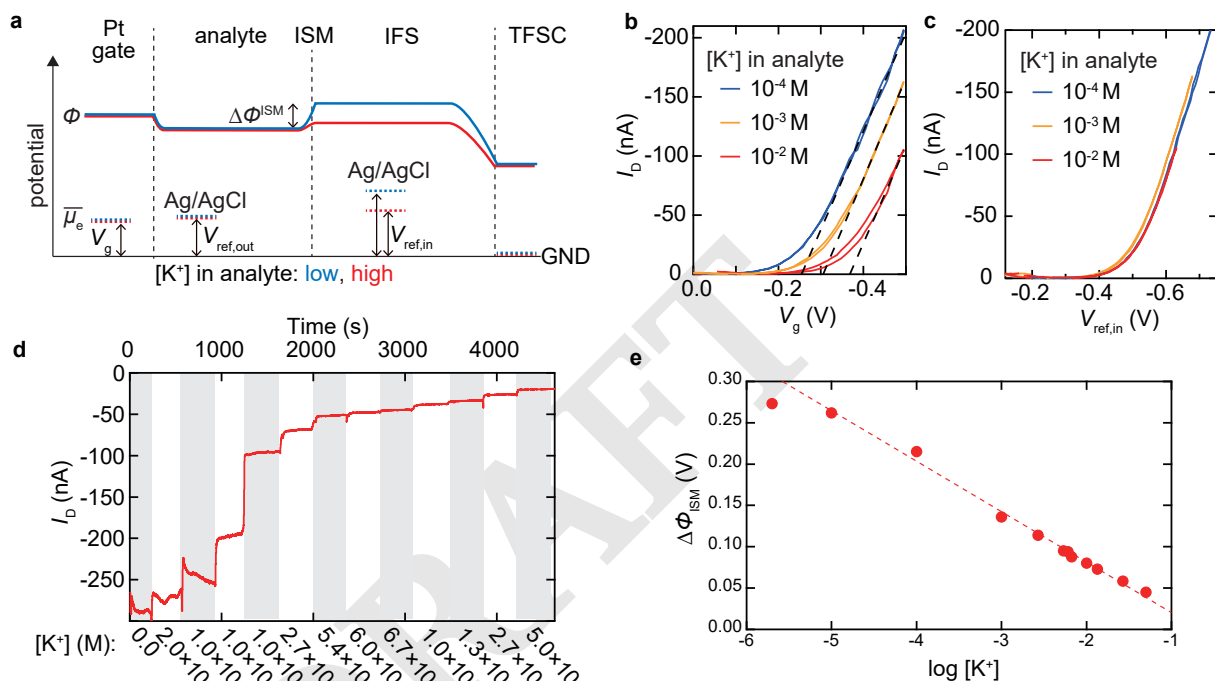


Fig. 2. K^+ sensing with an EDLT. (a) Illustration of sensing mechanism. The electric potential is shown in a solid line and the electrochemical potential of electrons (Fermi energy) is shown in dashed lines. GND denotes the ground level of the electronic system, which equals to the source electrode potential. $[K^+]$ is constant in IFS and varying in in analyte, where potentials for the cases with high and low $[K^+]$ in the analyte are illustrated. (b) Transistor characteristics with varying K^+ concentrations in the analyte plotted against V_g and (c) $V_{ref,in}$. V_d was -0.04 V. (d) Continuous measurements of I_d for varying K^+ concentrations with V_g of -0.4 V and V_d of -0.1 V. $[Na^+] + [K^+]$ was constant for this measurement. (e) The Nernst plot was obtained from EDLT measurements. Dashed line shows linear fitting with 61 mV dec^{-1} .

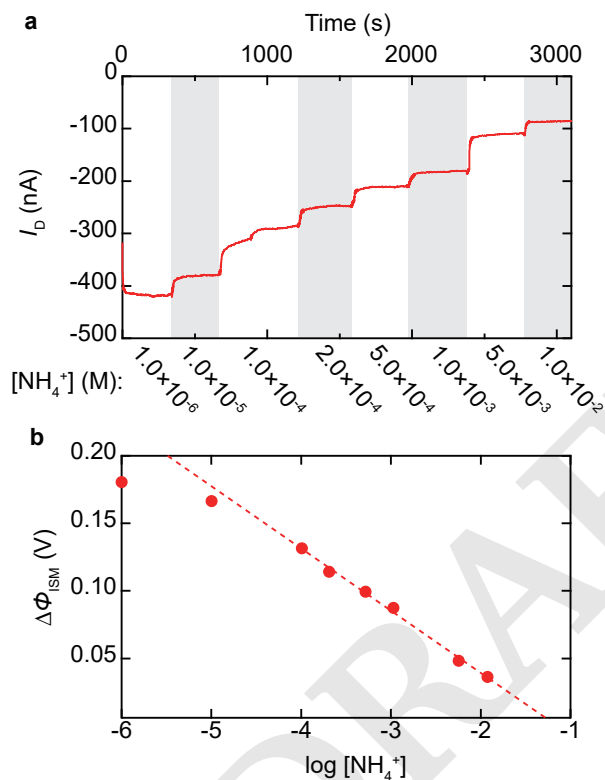


Fig. 3. NH_4^+ sensing with an EDLT. (a) Continuous measurements of I_d for varying NH_4^+ concentrations with V_g of -0.3 V and V_d of -0.1 V . No interfering ion was employed in this measurement. (b) The Nernst plot was obtained from EDLT measurements. The dashed line shows linear fitting with slope of 44 mV dec^{-1}

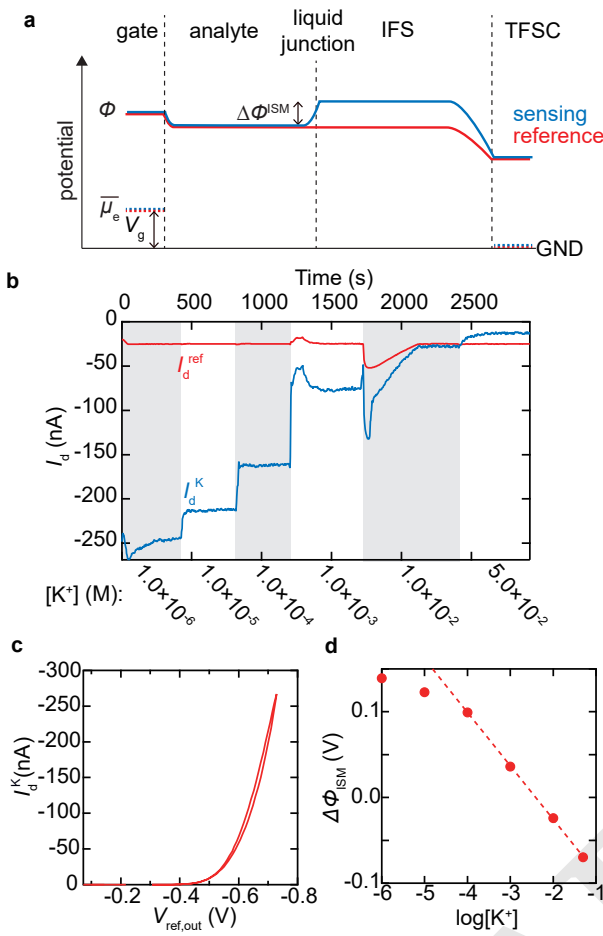


Fig. 4. Performance of combined sensing and reference EDLTs. (a) Illustration of sensing mechanism. The electric potential is shown in a solid line and the electrochemical potential of electrons (Fermi energy) is shown in dashed lines. Red lines show the potentials for the reference EDLT and blue lines show potentials for the sensing EDLT. GND denotes the ground level of the system, which equals to the source electrode potential. $[K^+]$ is constant in IFS and varying in analyte. (b) Continuous measurements of I_d for varying $[K^+]$ without using an RE. V_g was controlled so that I_d^{ref} becomes constant value. V_d was -50 mV. $[Na^+]$ was 0.1 M for this measurement. (c) Transistor characteristics of K^+ sensing EDLT plotted against electrode potential difference between source and Ag/AgCl. V_d was -50 mV. The analyte contained 0.05 M Na_2SO_4 and 0.1 mM K_2SO_4 . (d) The Nernst plot was obtained from sensing and reference EDLTs without using an RE. The dashed line shows linear fitting with slope of 62 mV dec⁻¹.